Proceeding Paper

Jakarta's 2020 New Year Flood Assessment with a Rainfall–Runoff–Inundation (RRI) Model †

Yeremia Immanuel Sihombing [1,*], Akbar Rizaldi [1], Mohammad Farid [1], N. Fajar Januriyadi [2] and Idham Riyando Moe [3]

1. Center for Coastal and Marine Development, Institute for Research and Community Services, Institut Teknologi Bandung, Jalan Ganesha No. 10, Kota Bandung 40132, Indonesia; akbar@ftsl.itb.ac.id (A.R.); mfarid@ftsl.itb.ac.id (M.F.)
2. Department of Civil Engineering, Pertamina University, Jalan Teuku Nyak Arief, RT.7/RW.8, Simprug, Kec. Kby. Lama, Kota Jakarta Selatan 12220, Indonesia; nurul.fj@universitaspertamina.ac.id
3. Directorate General of Water Resources, Ministry of Public Works and Housing, Jalan Pattimura No. 20, Kebayoran Baru, Jakarta Selatan 12110, Indonesia; idham.moe@gmail.com
* Correspondence: yeremia.sihombing97@gmail.com
† Presented at the 7th International Electronic Conference on Water Sciences, 15–30 March 2023; Available online: https://ecws-7.sciforum.net/.

Abstract: Floods hit Jakarta and several areas in the Ciliwung–Cisadane Watershed. The rain that occurred on 31 December 2019 stopped briefly and continued until 1 January 2020. As a result, several areas were flooded for several days. It is said that the rain that occurred was the largest in history. At least, the rainfall station at Halim Perdanakusuma Airport recorded rainfall with an intensity of 377 mm/day. That prompts a question about how much discharge was generated by the rainfall. This study was conducted to assess the flood discharge and the inundated area caused by the rain on 2020 New Year's Eve. The rainfall–runoff–inundation (RRI) model was utilized to simulate the flood discharge and inundation using the 1D–2D hydraulic–hydrology model. This model also calculated infiltration and subsurface flow with the Green–Ampt equation. In addition, the rainfall data used rain data recorded by the ground station, and the topography used SRTM data from the United States Geological Survey (USGS). Then, the flood discharge obtained from the model was compared with the flood return period. The return periods of the flood that were compared were at 2, 5, 10, 25, 50 and 100 years. The results showed that the flood that occurred on 1 January 2020 was larger than the flood with a return period of 100 years. This means that rainfall had the biggest effect on the flood, rather than other factors.

Keywords: flood; Jakarta; 2020; RRI

1. Introduction

Flooding is a natural process of a body of water, which rises to overflow land that is not normally submerged, due to high flow of runoff or sea-surge water [1–3]. There are several types of floods, including fluvial floods, pluvial floods and coastal floods [4–6]. Pluvial floods could be caused by the rain process, which produces an amount of water flow, on the surface, called runoff. Runoff is simply determined by rainfall, area of catchment and catchment response, which is represented by a runoff coefficient [7]. Many factors can cause flooding, including meteorological, geomorphological and anthropogenic factors [8–15]. Due to meandering river shape conditions, especially if the riverbed narrows throughout, a large discharge of water can derive an overflow [16]. Some places that previously did not experience floods have become areas affected by flooding due to changes in land use in the upstream areas [17,18]. In urban areas, flooding occurs due to illegal settlement and sedimentation, which reduce the capacities of rivers and channels [19–21]. In cold-climate regions, early spring snowmelt combined with heavy rainfall can also cause flooding [22].

Seawater levels rising and high rainfall, which are effects of climate change, are also causes of flooding in some areas [23–26]. Social behavior that occurs in the community can also indirectly have an impact on runoff: for example, urbanization. Urbanization will affect the land use of some areas, making changes in land cover that will affect runoff [27,28].

Jakarta was hit by flooding again in early 2020, on January 1st. One hundred and three locations were submerged by the flood around the provinces of DKI Jakarta and West Java, which are located in the Ciliwung–Cisadane Watershed [29]. Flooding occurred due to high rainfall intensity on 31 December 2019, exactly 1 day before. At least two of the eight stations around the DKI Jakarta area recorded rainfall of more than 300 mm; this is the highest rainfall of the last 25 years [30].

Flooding in the Ciliwung–Cisadane Watershed is not a new issue. It has happened since the 1660s [31]. An increase in discharge in the Ciliwung river was allegedly triggered by a change in the land use in the upstream area to become a tea plantation [32]. Some countermeasures to deal with increased runoff in the Ciliwung River have been carried out since the 1970s, and some have been implemented to date [33]. However, over time, as some areas began to develop, the problem of flooding in the Ciliwung–Cisadane Watershed became increasingly complex, and flooding still occurred.

The floods, which have not yet been solved, have caused several areas in the Ciliwung–Cisadane Watershed to still suffer from flooding. This has caused material and nonmaterial losses. These losses were not only caused by the size of the affected area but also due to the unpreparedness of the area in the face of disaster. The more prepared an area is in dealing with disasters, the more it will reduce the losses suffered [34]. This preparedness is not only related to the protection of an area against flooding but all the effort in that area in dealing with the flood disaster itself. This preparedness includes structural and nonstructural efforts [35]. Integration and sustainability of preparation, protection and the ability to respond effectively are the keys to resilience to flood disaster [36].

Many studies about the floods in the Ciliwung–Cisadane Watershed have been carried out, with different considerations. Climate change, land subsidence, land-use change and even social phenomena such as urbanization have been considered in several studies about flooding in the Ciliwung–Cisadane Watershed [37,38]. Future projection of flooding in the Ciliwung basin has been discussed in several studies as well. Moe et al. conducted a study related to the possibility of flooding in Jakarta, with scenarios caused by land subsidence combined with land-use changes [39,40]. Emam et al. showed how climate change and land-use change influence the flood behavior in Jakarta; it increased the peak flow of a 50-year return period in 2030 by 130% [41]. Januriyadi et al. not only conducted a study about future flooding but also analyzed the flood risk, due to climate change and urban development, for 2050 and showed that the risk has multiplied extremely [42].

Although many studies have been conducted about flooding in the Ciliwung–Cisadane Watershed, the occurrence of floods almost every year makes flooding still of interest to be investigated. To predict future changes is of great interest, but projecting current events to past predictions is also beneficial. The news related to Jakarta floods in the early 2020s, and moreover, the information that the rain that occurred was the most in history, startled Indonesia. The question is how large the flood discharge was due to that rain event, and to be more specific, which return period would have been equivalent to the coming flood on 1 January 2020. Today, it is not impossible to assess the flood after it happened. In 2018, Moe et al. conducted a rapid assessment to predict the affected area due to flooding in the Upper Citarum River Basin [43]. The aim of this study is to know the characteristics of the flood on 2020 New Year's Eve using rapid assessment.

2. Materials and Methods

2.1. Study Area

The study area was located at the Ciliwung–Cisadane Watershed, as shown in Figure 1. The watershed consists of 15 river basins, which accumulatively have an area of 5269.84 km². It administratively covers 3 provinces and 9 cities/municipalities, as follows: the Province

of DKI Jakarta (5 cities), Bogor, Depok, Bekasi and Tangerang. The study area was located between latitude 5°59′28″ S and latitude 6°47′18″ S and between longitude 106°24′45″ E and longitude 107°12′54″ E.
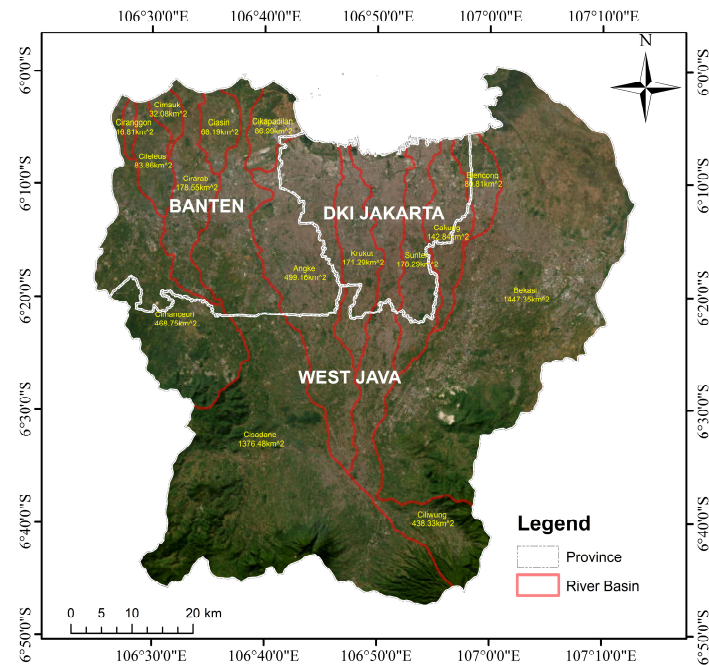

Figure 1. Study area.

2.2. Data

2.2.1. Precipitation Data

Precipitation data were collected from 24 rainfall stations in the Ciliwung–Cisadane Watershed during the flood event (Table 1). All of the rain stations are located around the study area, as shown in Figure 2a,b, which presents the rainfall distribution throughout the river area using the Inverse Distance Weighted Interpolation (IDW) method. The IDW method is the most frequently used deterministic method and can be applied for data whose distribution is characterized by a very large range [44]. From the data, the maximum rainfall during the studied event reached 376 mm. This condition is higher than the predicted rainfall for a 100-year return period in Halim Station, which was 340 mm [45].
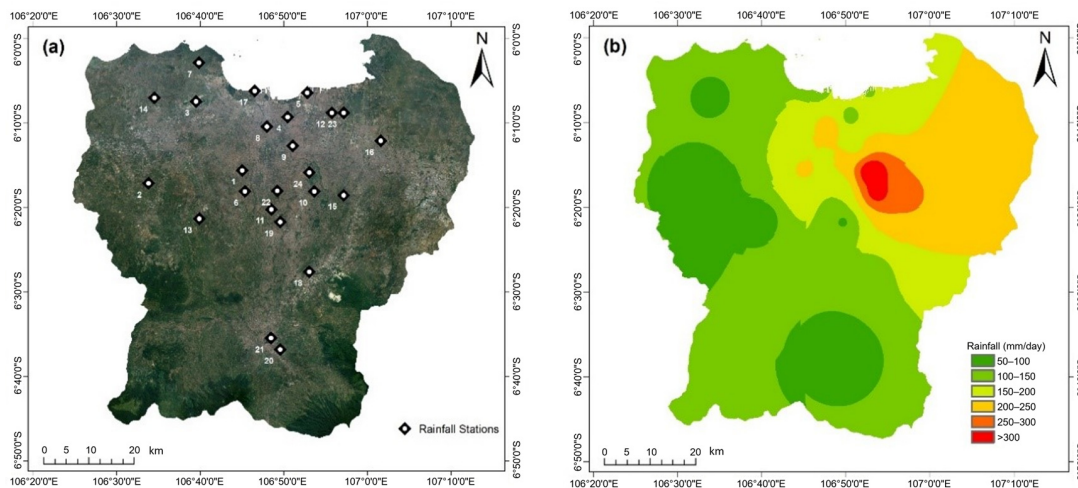

Figure 2. Rainfall datasets in the study area. (**a**) Rainfall station locations. (**b**) Rainfall distribution on 1 January 2020.

Table 1. List of rainfall stations.

No.	Rainfall Station	No.	Rainfall Station
1	Stasiun Klimatologi Tanggerang Selatan	13	AWS Puspitek
2	Stasiun Meteorologi Curug	14	ARG Sepatan
3	Stasiun Meteorologi Cengkareng	15	ARG Jatiasih
4	Stasiun Meteorologi Kemayoran	16	ARG Teluk Pucung
5	Stasiun Maritim Tanjung Priok	17	ARG Muara
6	Pos Hujan Bd Ciputat	18	ARG Jagorawi
7	Pos Hujan Teluk Naga	19	AWS UI
8	ARG Tomang	20	ARG Katulampa
9	ARG Manggarai	21	AWS IPB
10	AWW TMII	22	Pos Hujan Ragunan
11	ARG Ciganjur	23	Pos Hujan Rorotan
12	ARG Sukapura	24	TNI AU Halim

The predicted return-period rainfall was utilized as input in a calibrated model to determine the characteristics of various return periods of flooding. The calculation for return periods of rainfall was developed by Januriyadi et al. [42]. Our forecasting used a BMKG (Meteorological and Geophysical Institution of Indonesia) rainfall dataset for the period of 1986–2010 as a reference. The data were distributed throughout the study area, as presented in Figure 3. Compared with the rainfall that occurred on 1 January, the maximum rainfall of that event exceeded the maximum data in a 100-year period, which corresponds well with the previous study.
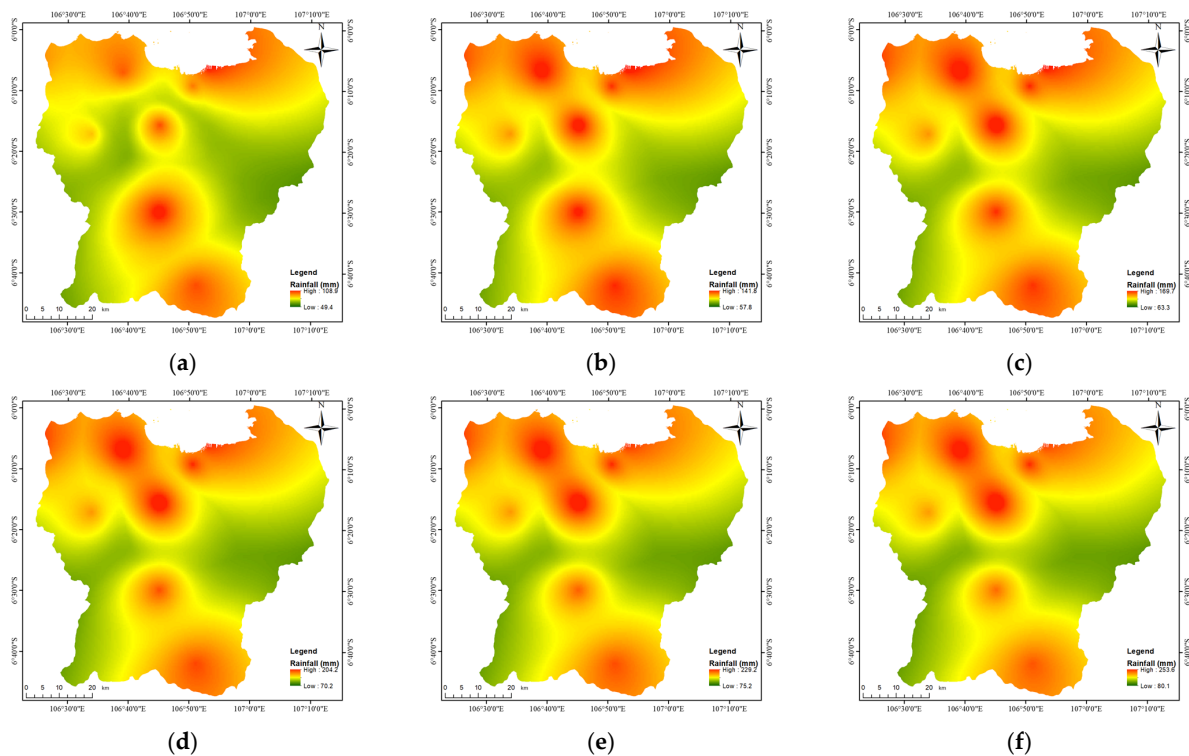

Figure 3. Rainfall return-period datasets. (**a**) Rainfall return-period of 2 years. (**b**) Rainfall return-period of 5 years. (**c**) Rainfall return-period of 10 years. (**d**) Rainfall return-period of 25 years. (**e**) Rainfall return-period of 50 years. (**f**) Rainfall return-period of 100 years.

2.2.2. Topography

The topography data was derived from the Digital Elevation Model (DEM) obtained from the Shuttle Radar Topography Mission (SRTM). The data was open-source data provided by the United States Geological Survey (USGS). For the SRTM, the vertical accuracy was 16 m for a 90% confidence level [46].

Figure 4 presents the topographical conditions of the Ciliwung–Cisadane Watershed. The resolution of the DEM that was used in this calculation was based on 1 arc second, or about 30 m. Nevertheless, the resolution was scaled up to 100 m due to computational issues. The numbers of rows and columns of pixels are 885 and 891. The upscaling of the DEM resolution increased the topography index (TI) of the DEM because of the nesting process of several grids with different TIs into one grid with one TI [47]. The consequences were areas or grids that should have been submerged becoming dry areas, and vice versa.
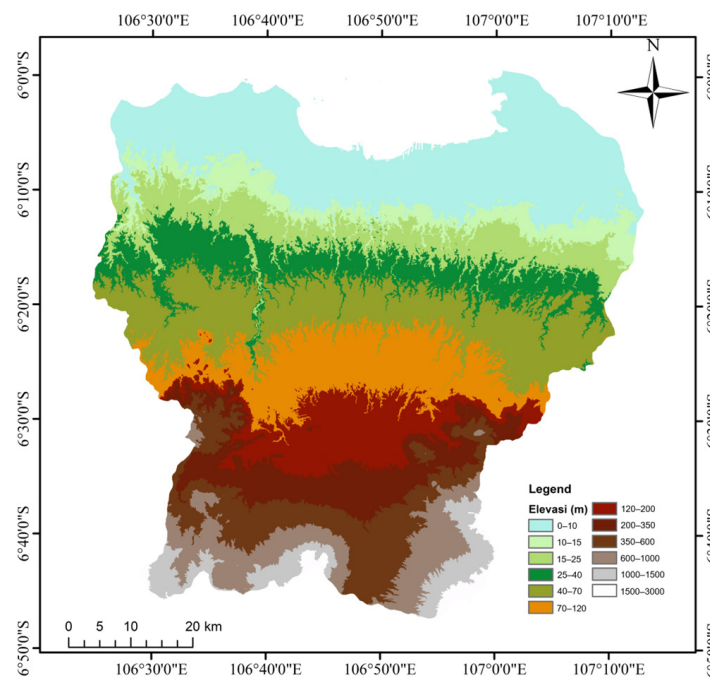

Figure 4. Digital Elevation Model (DEM) of the Ciliwung–Cisadane Watershed.

2.2.3. Land Cover

Land cover data was obtained from the Global Land Cover Characterization Version 2 (GLCC-V2). This database was developed by The U.S. Geological Survey (USGS), the University of Nebraska–Lincoln (UNL) and the European Commission's Joint Research Centre (JRC) in 1992. The land-cover projection had 1 km nominal spatial resolution and unique geographic elements. The land classification for this model has been simplified from the GLCC-V2 for calculation purposes (Figure 5).

Each land-cover classification has different characteristics in the model, based on soil conditions, as presented in Table 2. In this model, the river was distinguished from other water bodies. The river location was autogenerated by the RRI model from the Digital Elevation Model.
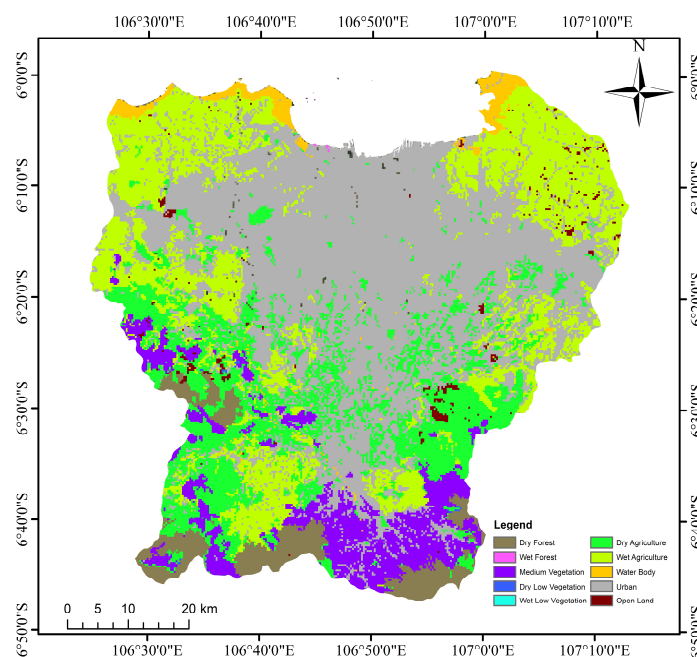
Figure 5. Land cover of the Ciliwung–Cisadane Watershed.

Table 2. The characteristics of the land cover.

Parameter	Land Cover		
	Clay	**Loam**	**Sandy Clay Loam**
Soil Depth (m)	1	1	1
Porosity (-)	0.475	0.463	0.398
k_v (m/s)	$0–8.33 \times 10^{-8}$	$0–9.44 \times 10^{-7}$	$0–4.17 \times 10^{-7}$
S_f	0.361	0.089	0.219
k_a (m/s)	0–0.3	0–0.3	0–0.3
Unsat. Porosity (-)	0	0	0
Beta	8	8	8

2.3. Rainfall–Runoff–Inundation (RRI) Model

The rainfall–runoff–inundation (RRI) model is a two-dimensional model with a simplified equation. This model is capable of simulating rainfall–runoff and flood inundation at the same time; it was also designed to be used immediately after a disaster and it can be useful as a tool to analyze large-scale flooding as well [48]. In addition, this model assumes that the river channel location is in the same grid cells as the slope. A river channel is considered a centerline in a grid cell. It indicates an extra flow path between the grid cells and the actual river course. On the other hand, the slope cells function as the two-dimensional simulation area of the lateral flow. Hence, there are two water depths for slope grid cells in water channels, i.e., of the channel and of the slope (floodplain) itself.

The inflow–outflow interaction between the river and the slope is based on different overflowing formulae. The calculation depends on water-level and levee-height conditions. This model was generated based on mass-balance Equation (1) for governing the equation of flow rate. The momentum equation was derived from the governing equation of the model in the x direction (Equation (2)) and the y direction (Equation (3)):

$$\frac{\partial h}{\partial t} + \frac{\partial q_x}{\partial x} + \frac{\partial q_y}{\partial y} = r - f \tag{1}$$

$$\frac{\partial q_x}{\partial t} + \frac{\partial u q_x}{\partial x} + \frac{\partial v q_x}{\partial y} = -g\,h\,\frac{\partial H}{\partial x} - \frac{\tau_x}{\rho_w} \tag{2}$$

$$\frac{\partial q_y}{\partial t} + \frac{\partial u q_y}{\partial x} + \frac{\partial v q_y}{\partial y} = -g\,h\,\frac{\partial H}{\partial y} - \frac{\tau_y}{\rho_w} \tag{3}$$

where h is the height of the water from the local surface; q_x and q_y are the unit width discharges in the x and y directions, respectively; u and v are the flow velocities in the x and y directions, respectively; r is rainfall intensity; H is the height of water from the datum; ρw is the density of the water, g is gravitational acceleration; and τ_x and τ_y are the shear stresses in the x and y directions, respectively.

The RRI model separates the calculations of the discharge and the hydraulic gradient relationship. Hence, simulations of surface and subsurface flow proceed in the same algorithm. In addition, kinematic-rainfall–runoff-wave and diffusive-wave approximation are also derived in this model. The kinematic wave is calculated with the assumption that the water-surface slope is the hydraulic gradient. On the other hand, diffusion-stream approximation is utilized to form the streamflow equation.

The calibration process was carried out via a simulation of the flood events on 1 January. Then, the inundation area from the simulation was compared with the inundation map obtained from remote sensing by satellites at the same time. The model would have been well-calibrated if the result showed similarities to the inundation obtained from the remote sensing.

3. Results and Discussion

3.1. Model Calibration

The model was calibrated before being used to simulate the return-period flood. It was calibrated with a flood event that occurred on 1 January 2020. The simulation calculated the distribution of flood inundation with the condition of maximum water depth and compared it to the inundated area's satellite data at the same event (Figure 6). Figure 6 shows the comparison of the simulated flood inundation and the flood inundation from Sentinel 1A acquired on 2 January 2020. The flood inundation from Sentinel 1A was generated using an algorithm that was proposed by Chini et al. [49]. The algorithm can detect flood water not only on bare soil but also in urban regions. Even though the Sentinel 1A data was acquired a day after the flood event, some inundation still remained on the land. The results shows similar inundation in the northeast part between the simulation and satellite data, whereas in the middle part, near the ocean, the figure shows that the simulated inundation areas are larger than in the satellite data because the flood waters in the urban area of Jakarta receded on 2 January 2020.
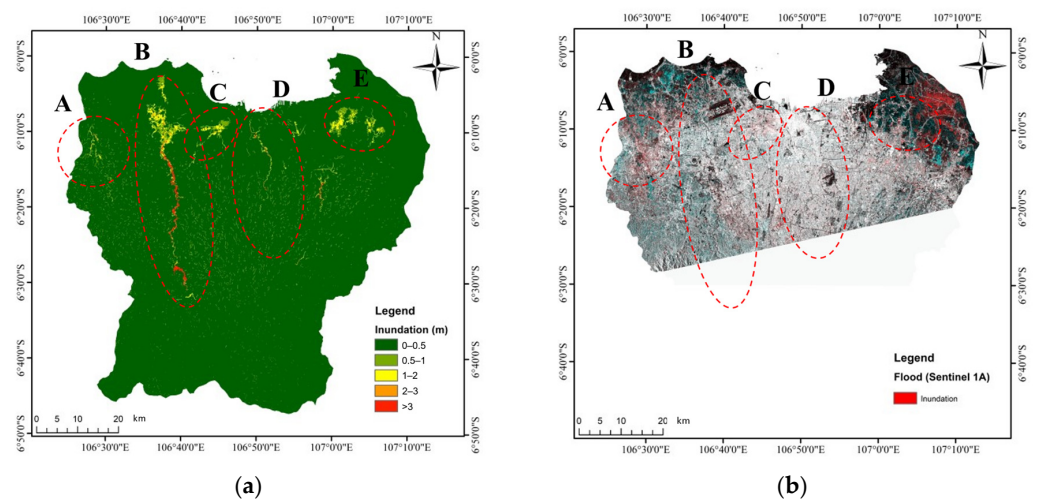

(a)　　　　　　　　　　　　　　　(b)

Figure 6. Rapid assessment of Jakarta flood inundation: (**a**) simulated 1 January flood inundation and (**b**) flood inundation data from Sentinel 1A acquired on 2 January 2020.

The inundation in this model consisted of local inundation and large-scale inundation. Local inundation was defined as local water depth that was barely moving. Accordingly, this type of inundation has a limited range of area and shallow water depth. On the other hand, large-scale inundation is water depth that was growing around the river with a wide range of areas.

Circle A, B, C, D and E represent large-scale inundation during the simulation period. The locations of the circles are in the Cimanceuri, Cisadane, Angke, Ciliwung and Bekasi River Basins, respectively. Table 3 shows the approximation of the total affected area due to river inundation. The total area of river inundation was approximately 106.54 km^2. Hence, the percentage of river inundation area during this event was 56.51% of the total inundation area.

Table 3. Large-scale inundation area.

Location	River Basin	Inundation Area (km^2)	Affected City(ies)
A	Cimanceuri	6.3	Tanggerang
B	Cisadane	51.05	Tanggerang
C	Angke	11.9	West Jakarta
D	Ciliwung	5.03	East Jakarta, South Jakarta, Central Jakarta
E	Bekasi	32.26	Bekasi

3.2. Model Application

The model that was calibrated was used to perform the return-period analysis of the flood. The flood return periods were simulated in mostly the same conditions as the main simulation. Nevertheless, the precipitation used as input in these simulations was modified for rainfall return periods that were forecast from historical rainfall data. The periods of rainfall that were used in this calculation were 2 years, 5 years, 10 years, 25 years, 50 years and 100 years. The results of these simulations are shown in Figure 7. Most of the large-scale inundation in each return period was found in the same locations, i.e., the Cimanceuri, Cisadane, Angke, Ciliwung and Bekasi River Basins. Therefore, the location of the large-scale inundation was the same as in the main simulation.

The area and volume of the inundation were calculated in the flood return period simulation. Then, the area and volume of the inundation were compared with the inundation characteristics of the flood that occurred on 1 January 2020. Table 4 shows that the closest return-period flood area to the flood on 1 January was the period with 100 yearly floods. The inundated areas of both flood maps were quite similar (Figure 8). This strengthens the evidence that the flood that occurred on 1 January was a flood with a return period of 100 years, whereas the rainfall on that day was greater than the rainfall for a return period of 100 years. The flood may not have been as large as the rainfall due to the spatial distribution of rainfall. The variability of rainfall spatial distribution could have affected the amount of flood discharge, which generates different flooding [50,51].
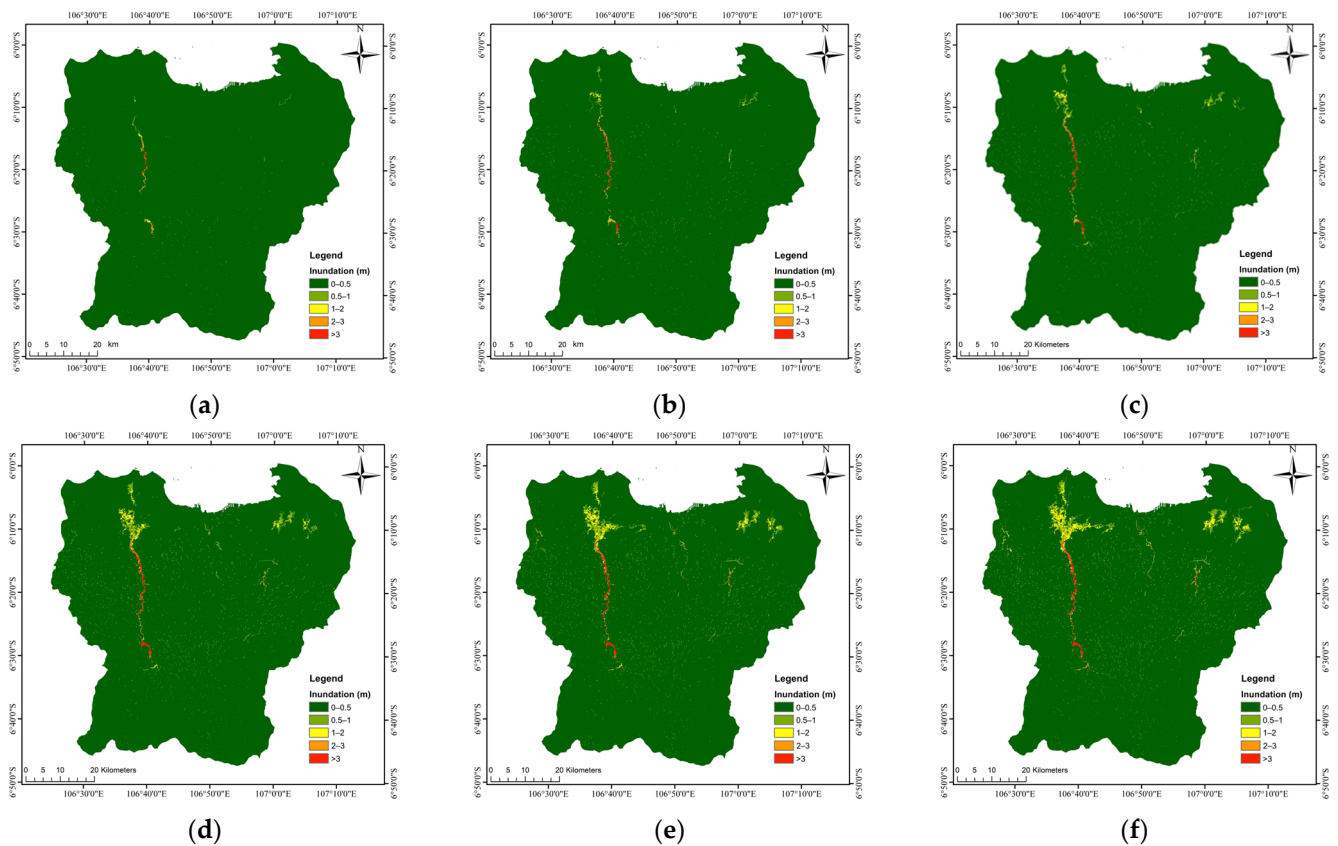
Figure 7. The inundation of flood return periods. (**a**) Flood return period of 2 years. (**b**) Flood return period of 5 years. (**c**) Flood return period of 10 years. (**d**) Flood return period of 25 years. (**e**) Flood return period of 50 years. (**f**) Flood return period of 100 years.

Table 4. The characteristics of flood return periods.

Flood Simulation	Volume (1000 m^3)	Max. Discharge (m^3/s)
Return Period of 2 Years	16,475	199.75
Return Period of 5 Years	22,059	260.88
Return Period of 10 Years	25,797	297.85
Return Period of 25 Years	30,397	340.95
Return Period of 50 Years	33,450	365.67
Return Period of 100 Years	36,355	389.97
Jakarta Flood	40,204	420.76

The flood discharge was calculated for the main model and the flood return period. It was measured with RRI hydro calculation at Water Gate Manggarai on the Ciliwung River (106°12′27.48″ S and 106°50′54.55″ E). The maximum discharge of each model is presented in Table 4. The discharge of the main model was compared with floods with 2-, 5-, 10-, 25-, 50- and 100-year return periods (Figure 9). The maximum discharge of the main model exceeded the 100-year return period. Therefore, the main model corresponded better with the rain-gauge data, which was more than the 100-year return-period rain data.
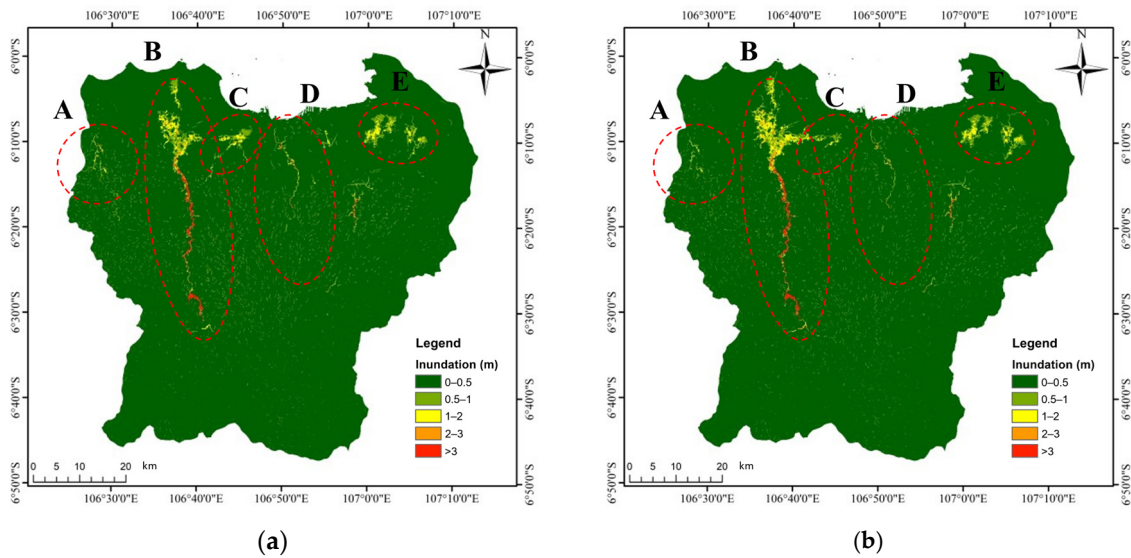
Figure 8. The comparison between (**a**) the 100-year flood return period and (**b**) the flood on 1 January 2020.
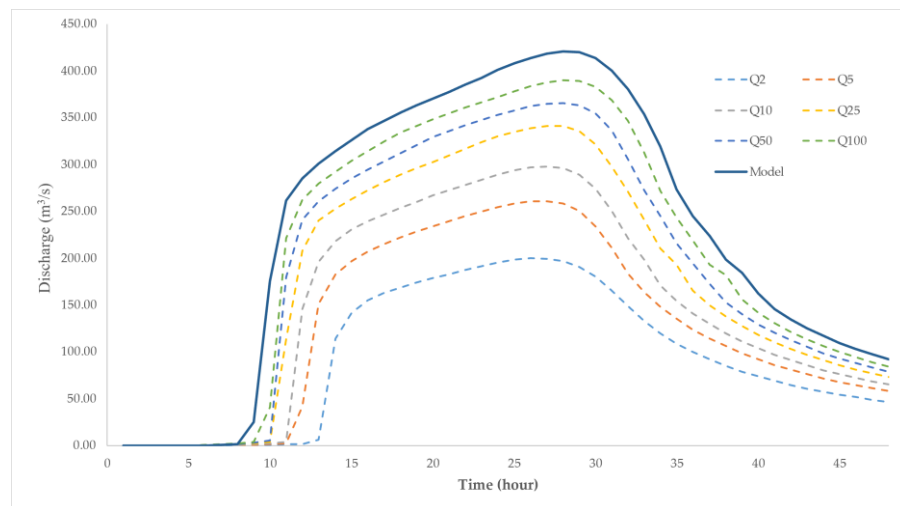

Figure 9. Discharge at Water Gate Manggarai.

4. Conclusions

This study attempted to conduct a rapid assessment of the flood on 1 January 2020 in Jakarta and several areas of the Ciliwung–Cisadane Watershed. This study was conducted to determine the return period of the flood that occurred. The rainfall–runoff–inundation (RRI) model is a distributed model that is able to simulate rainfall–runoff and flooding simultaneously. The model based on the inundation map from remote-sensing satellites was calibrated with ground-station rainfall data. The resolution of the Digital Elevation Model (DEM), which was too high, hindered the simulation process; it made it necessary for the resolution of the DEM to be decreased. The DEM was upscaled; then, the grid size was changed from 30 m to 100 m. After the model was calibrated, a return-period flood model was performed with a return-period rainfall input. There were six return periods of rainfall being simulated: 2, 5, 10, 25, 50 and 100 years.

The discharge and inundation areas of all return periods were compared with the simulation of the flood on 1 January. The comparison showed that the discharge extent on 1 January exceeded the discharge for a return period of 100 years. This result corresponds with the rain recorded at several rainfall stations, which surpassed the 100-year rainfall return period. Thus, there are several conclusions. First, the flood that occurred on 1

January 2020 was superior to a 100-year return period of flooding. Second, the rainfall, which was the most in history, was the main effect of this flood because it exceeded the 100-year return period of rainfall.

In this study, the DEM implemented in this model had a low resolution because of the limitation of data sources. In addition, the model needed to be compared with the existing discharge during the flood. These conditions need to be considered in future research.

Author Contributions: Conceptualization, M.F., N.F.J. and I.R.M.; methodology, M.F., N.F.J. and I.R.M.; software, Y.I.S. and N.F.J.; validation, Y.I.S. and A.R.; formal analysis, Y.I.S. and A.R; investigation, Y.I.S. and A.R.; resources, M.F. and I.R.M.; data curation, Y.I.S. and A.R.; writing—original draft preparation Y.I.S., A.R. and N.F.J.; writing—review and editing, M.F. and I.R.M.; visualization, Y.I.S. and A.R.; supervision, M.F. and I.R.M.; project administration, M.F. and I.R.M.; funding acquisition, M.F. and I.R.M. All authors have read and agreed to the published version of the manuscript.

Institutional Review Board Statement: Not applicable.

Informed Consent Statement: Not Applicable.

Data Availability Statement: Data is unavailable.

Conflicts of Interest: The authors declare no conflict of interest.

References

1. Chow, V.T.; Maidment, D.R.; Mays, L.W. *Applied Hydrology*; McGraw-Hill Book Company: New York, NY, USA, 1988. Available online: https://ponce.sdsu.edu/Applied_Hydrology_Chow_1988.pdf (accessed on 1 February 2023).
2. Penning-Rowsell, E.C.; Ward, R. Floods: A Geographical Perspective. *Geogr. J.* **1980**, *146*, 139. [CrossRef]
3. Webster, T.L.; Forbes, D.L.; Dickie, S.; Shreenan, R. Using topographic lidar to map flood risk from storm-surge events for Charlottetown, Prince Edward Island, Canada. *Can. J. Remote Sens.* **2004**, *30*, 64–76. [CrossRef]
4. Merz, B.; Hall, A.J.; Disse, M.; Schumann, A.H. Fluvial flood risk management in a changing world. *Nat. Hazards Earth Syst. Sci.* **2010**, *10*, 509–527. [CrossRef]
5. Zhou, Q.; Mikkelsen, P.S.; Halsnæs, K.; Arnbjerg-Nielsen, K. Framework for economic pluvial flood risk assessment considering climate change effects and adaptation benefits. *J. Hydrol.* **2012**, *414–415*, 539–549. [CrossRef]
6. Ganguli, P.; Merz, B. Extreme Coastal Water Levels Exacerbate Fluvial Flood Hazards in Northwestern Europe. *Sci. Rep.* **2019**, *9*, 13165. [CrossRef]
7. Ferreira, S.; Ghimire, R. Forest cover, socioeconomics, and reported flood frequency in developing countries. *Water Resour. Res.* **2012**, *48*, W08529. [CrossRef]
8. Li, F.; Wang, L.; Zhao, Y. Evolvement rules of basin flood risk under low-carbon mode. Part I: Response of soil organic carbon to land use change and its influence on land use planning in the Haihe basin. *Environ. Monit. Assess.* **2017**, *189*, 377. [CrossRef]
9. Maes, J.; Molombe, J.M.; Mertens, K.; Parra, C.; Poesen, J.; Che, V.B.; Kervyn, M. Socio-political drivers and consequences of landslide and flood risk zonation: A case study of Limbe city, Cameroon. *Environ. Plan. C Politics Space* **2019**, *37*, 707–731. [CrossRef]
10. Mahmoud, S.H.; Gan, T.Y. Urbanization and climate change implications in flood risk management: Developing an efficient decision support system for flood susceptibility mapping. *Sci. Total Environ.* **2018**, *636*, 152–167. [CrossRef]
11. Blume, T.; Zehe, E.; Bronstert, A. Rainfall—Runoff response, event-based runoff coefficients and hydrograph separation. *Hydrol. Sci. J.* **2007**, *52*, 843–862. [CrossRef]
12. Baker, V.R.; Pickup, G. Flood geomorphology of the Katherine Gorge, Northern Territory, Australia. *Geol. Soc. Am. Bull.* **1987**, *98*, 635. [CrossRef]
13. Bauer, B.O.; Baker, V.R.; Kochel, R.C.; Patton, P.C. Flood Geomorphology. *Geogr. Rev.* **1990**, *80*, 341. [CrossRef]
14. Texier, P. Floods in Jakarta: When the extreme reveals daily structural constraints and mismanagement. *Disaster Prev. Manag.* **2008**, *17*, 358–372. [CrossRef]
15. Lee, M.-H.; Bae, D.-H. Climate Change Impact Assessment on Green and Blue Water over Asian Monsoon Region. *Water Resour. Manag.* **2015**, *29*, 2407–2427. [CrossRef]
16. Baker, V.R. Stream-Channel Response to Floods, with Examples from Central Texas. *Geol. Soc. Am. Bull.* **1977**, *88*, 1057–1071. [CrossRef]
17. Dasanto, B.D.; Pramudya, B.; Boer, R.; Suharnoto, Y. Effects of Forest Cover Change on Flood Characteristics in the Upper Citarum Watershed. *J. Manaj. Hutan Trop. (J. Trop. For. Manag.)* **2014**, *20*, 141–149. [CrossRef]

18. Farid, M.; Mano, A.; Udo, K. Modeling flood runoff response to land cover change with rainfall spatial distribution in urbanized catchment. *J. Jpn. Soc. Civ. Eng. Ser. B1 (Hydraul. Eng.)* **2011**, *67*, I_19–I_24. [CrossRef]

19. Rosso, R.; Rulli, M.C. An integrated simulation method for flash-flood risk assessment: 2. Effects of changes in land-use under a historical perspective. *Hydrol. Earth Syst. Sci.* **2002**, *6*, 285–294. [CrossRef]

20. Lane, S.N.; Reid, S.C.; Tayefi, V.; Yu, D.; Hardy, R.J. Reconceptualising coarse sediment delivery problems in rivers as catchment-scale and diffuse. *Geomorphology* **2008**, *98*, 227–249. [CrossRef]

21. Rizaldi, A.; Moe, I.R.; Farid, M.; Aribawa, T.M.; Bayuadji, G.; Sugiharto, T. Study of flood characteristic in Cikalumpang River by using 2D flood model. *MATEC Web Conf.* **2019**, *270*, 04010. [CrossRef]

22. Zaghloul, M.S.; Ghaderpour, E.; Dastour, H.; Farjad, B.; Gupta, A.; Eum, H.; Achari, G.; Hassan, Q.K. Long Term Trend Analysis of River Flow and Climate in Northern Canada. *Hydrology* **2022**, *9*, 197. [CrossRef]

23. Karim, M.F.; Mimura, N. Impacts of climate change and sea-level rise on cyclonic storm surge floods in Bangladesh. *Glob. Environ. Change* **2008**, *18*, 490–500. [CrossRef]

24. Hallegatte, S.; Ranger, N.; Mestre, O.; Dumas, P.; Corfee-Morlot, J.; Herweijer, C.; Wood, R.M. Assessing climate change impacts, sea level rise and storm surge risk in port cities: A case study on Copenhagen. *Clim. Change* **2010**, *104*, 113–137. [CrossRef]

25. Darsan, J.; Asmath, H.; Jehu, A. Flood-risk mapping for storm surge and tsunami at Cocos Bay (Manzanilla), Trinidad. *J. Coast. Conserv.* **2013**, *17*, 679–689. [CrossRef]

26. Buchanan, M.K.; Kopp, R.E.; Oppenheimer, M.; Tebaldi, C. Allowances for evolving coastal flood risk under uncertain local sea-level rise. *Clim. Change* **2016**, *137*, 347–362. [CrossRef]

27. Du, J.; Qian, L.; Rui, H.; Zuo, T.; Zheng, D.; Xu, Y.; Xu, C.-Y. Assessing the effects of urbanization on annual runoff and flood events using an integrated hydrological modeling system for Qinhuai River basin, China. *J. Hydrol.* **2012**, *464–465*, 127–139. [CrossRef]

28. Aich, V.; Liersch, S.; Vetter, T.; Fournet, S.; Andersson, J.C.; Calmanti, S.; van Weert, F.H.; Hattermann, F.F.; Paton, E.N. Flood projections within the Niger River Basin under future land use and climate change. *Sci. Total Environ.* **2016**, *562*, 666–677. [CrossRef]

29. BNPB Editorial. Hujan Ekstrem Penyebab Banjir Jakarta. Available online: https://bnpb.go.id/berita/hujan-ekstrem-penyebab-banjir-jakarta (accessed on 16 May 2020).

30. Biro Komunikasi Publik Kementrian PUPR. Menteri Basuki Siapkan Langkah Penanganan Banjir di Jakarta dan Sekitarnya. Available online: https://pu.go.id/berita/view/17794/menteri-basuki-siapkan-langkah-penanganan-banjir-di-jakarta-dan-sekitarnya (accessed on 16 May 2020).

31. Caljouw, M.; Nas, P.J.; Pratiwo, M. Flooding in Jakarta: Towards a blue city with improved water management. *J. Humanit. Soc. Sci. Southeast Asia* **2009**, *161*, 454–484. [CrossRef]

32. Kurniawan, B.E.; Corps, M. Adapting cities to climate variability and change: Balance between community engagement and supporting facilitation roles of the local government to reduce the impact of climate change. In Proceedings of the Human(e) Settlements: The Urban Challenge Conference, Johannesburg, South Africa, 17–21 September 2012.

33. Octavianti, T.; Charles, K. The evolution of Jakarta's flood policy over the past 400 years: The lock-in of infrastructural solutions. *Environ. Plan. C Politics Space* **2019**, *37*, 1102–1125. [CrossRef]

34. Miceli, R.; Sotgiu, I.; Settanni, M. Disaster preparedness and perception of flood risk: A study in an alpine valley in Italy. *J. Environ. Psychol.* **2008**, *28*, 164–173. [CrossRef]

35. Petry, B. Keynote Lecture: Coping with Floods: Complementarity of Structural and Non-Structural Measures. In *Flood Defence*; Science Press: New York, NY, USA, 2002; pp. 60–70.

36. Hadihardaja, I.K.; Kuntoro, A.A.; Farid, M. Flood Resilience for Risk Management: Case Study of River Basin in Indonesia. *Glob. Asp.* **2013**, *3*, 16–19.

37. Budiyono, Y.; Aerts, J.C.J.H.; Tollenaar, D.; Ward, P.J. River flood risk in Jakarta under scenarios of future change. *Nat. Hazards Earth Syst. Sci.* **2016**, *16*, 757–774. [CrossRef]

38. Mishra, B.K.; Emam, A.R.; Masago, Y.; Kumar, P.; Regmi, R.K.; Fukushi, K. Assessment of future flood inundations under climate and land use change scenarios in the Ciliwung River Basin, Jakarta. *J. Flood Risk Manag.* **2017**, *11*, S1105–S1115. [CrossRef]

39. Moe, I.R.; Kure, S.; Januriyadi, N.F.; Farid, M.; Udo, K.; Kazama, S.; Koshimura, S. Effect of land subsidence on flood inundation in Jakarta, Indonesia. *J. Jpn. Soc. Civ. Eng. Ser. G (Environ. Res.)* **2016**, *72*, I_283–I_289. [CrossRef]

40. Moe, I.R.; Kure, S.; Januriyadi, N.F.; Farid, M.; Udo, K.; Kazama, S.; Koshimura, S. Future projection of flood inundation considering land-use changes and land subsidence in Jakarta, Indonesia. *Hydrol. Res. Lett.* **2017**, *11*, 99–105. [CrossRef]

41. Emam, A.R.; Mishra, B.K.; Kumar, P.; Masago, Y.; Fukushi, K. Impact Assessment of Climate and Land-Use Changes on Flooding Behavior in the Upper Ciliwung River, Jakarta, Indonesia. *Water* **2016**, *8*, 559. [CrossRef]

42. Januriyadi, N.F.; Kazama, S.; Moe, I.R.; Kure, S. Evaluation of future flood risk in Asian megacities: A case study of Jakarta. *Hydrol. Res. Lett.* **2018**, *12*, 14–22. [CrossRef]

43. Moe, I.R.; Rizaldi, A.; Farid, M.; Moerwanto, A.S.; Kuntoro, A.A. The use of rapid assessment for flood hazard map development in upper citarum river basin. *MATEC Web Conf.* **2018**, *229*, 04011. [CrossRef]

44. Bronowicka-Mielniczuk, U.; Mielniczuk, J.; Obroślak, R.; Przystupa, W. A Comparison of Some Interpolation Techniques for Determining Spatial Distribution of Nitrogen Compounds in Groundwater. *Int. J. Environ. Res.* **2019**, *13*, 679–687. [CrossRef]

45. Liu, J.; Doan, C.D.; Liong, S.-Y.; Sanders, R.; Dao, A.T.; Fewtrell, T. Regional frequency analysis of extreme rainfall events in Jakarta. *Nat. Hazards* **2015**, *75*, 1075–1104. [CrossRef]

46. Jarvis, A.; Rubiano, J.; Nelson, A.; Farrow, A.; Mulligan, M. *Practical Use of SRTM Data in the Tropics—Comparisons with Digital Elevation Models Generated from Cartographic Data*; Centro Internacional de Agricultura Tropical (CIAT): Cali, Colombia, 2004.

47. Zhang, H.; Li, Z.; Saifullah, M.; Li, Q.; Li, X. Impact of DEM Resolution and Spatial Scale: Analysis of Influence Factors and Parameters on Physically Based Distributed Model. *Adv. Meteorol.* **2016**, *2016*, 8582041. [CrossRef]

48. Sayama, T.; Ozawa, G.; Kawakami, T.; Nabesaka, S.; Fukami, K. Rainfall–runoff–inundation analysis of the 2010 Pakistan flood in the Kabul River basin. *Hydrol. Sci. J.* **2012**, *57*, 298–312. [CrossRef]

49. Chini, M.; Pelich, R.; Pulvirenti, L.; Pierdicca, N.; Hostache, R.; Matgen, P. Sentinel-1 InSAR Coherence to Detect Floodwater in Urban Areas: Houston and Hurricane Harvey as a Test Case. *Remote Sens.* **2019**, *11*, 107. [CrossRef]

50. Ogden, F.L.; Sharif, H.O.; Senarath, S.U.S.; Smith, J.A.; Baeck, M.L.; Richardson, J.R. Hydrologic analysis of the Fort Collins, Colorado, flash flood of 1997. *J. Hydrol.* **2000**, *228*, 82–100. [CrossRef]

51. Arnaud, P.; Bouvier, C.; Cisneros, L.; Dominguez, R. Influence of rainfall spatial variability on flood prediction. *J. Hydrol.* **2002**, *260*, 216–230. [CrossRef]